LAWRENCE
LIVERMORE
NATIONAL
LABORATORY

LLNL-JRNL-417813

Carbon nanotube devices controlled by an ion pump.

Shih-Chieh Huang, Alexander Artyukhin, Nipun Misra, Julio Martinez, Pieter Stroeve, Costas Grigoropoulos, Jiann Wen Ju, Aleksandr Noy

October 9, 2009

Nano Letters

Disclaimer

Carbon nanotube devices controlled by an ion pump

Shih-Chieh J. Huang,[1,2] Alexander B. Artyukhin,[1,3,5] Nipun Misra,[1,4] Julio A. Martinez,[1,3] Pieter A. Stroeve,[3] Costas P. Grigoropoulos,[4] Jiann-Wen W. Ju,[2] and Aleksandr Noy[1,]*

[1] Molecular Biophysics and Functional Nanostructures Group, Physical and Life Sciences Directorate, Lawrence Livermore National Laboratory, Livermore, CA, USA

[2] Department of Civil Engineering, University of California Los Angeles, Los Angeles, CA

[3] Department of Chemical Engineering and Materials Science, University of California Davis, Davis, CA

[4] University of California Berkeley, Berkeley, CA

[5] Current address: Department of Pharmacology, University of Texas Southwestern Medical Center, Dallas, TX

[*]Address correspondence to AN (***noy1@llnl.gov***)

Abstract.

Biological systems have developed protein machines that function with remarkable complexity and sophistication. Integrating these machines into artificial hybrid circuits could increase capabilities and performance of nanodevices. We report a hybrid bionanoelectronic device in which a membrane ion pump, Na^+/K^+-ATPase, controls the output of a single carbon nanotube transistor. When we embedded ion pump molecules in the lipid bilayer covering the carbon nanotube, ATP-dependent protein activity increased the transistor output current by up to 40%. Specific Na^+/K^+-ATPase inhibitors suppress these current modulations. Further investigation showed that the ion pump gates the carbon nanotube by shifting the pH of the thin water layer between the lipid bilayer and nanotube surface. This device configuration provides a versatile and general bionanoelectronic platform that can incorporate other membrane proteins.

Living cells employ a large number of molecular machines that perform sophisticated tasks and functions that are critical for cell survival and proliferation. Some of these biomolecules have evolved to serve as structural elements, while others are critical for transmitting or storing information or maintaining intracellular environment and energy balance. Molecular machines play a vital role in DNA assembly (*1*), defect recognition and repair (*2, 3*), cargo transport (*4, 5*) and selection (*6, 7*), and ion balance maintenance (*8*). Great precision, efficiency, and accuracy of these biomolecules make them an attractive choice for incorporation into man-made structures to introduce new functionality and improve device performance (*9-11*). Carbon nanotube (CNT) devices could be particularly

promising candidates for building an inorganic platform for such integration given their ability to operate in physiological conditions, high sensitivity, and size scale suitable for working with individual biomolecules (*12, 13*). At the same time hydrophobic CNT surfaces do not represent a natural environment for most biomolecules and often have strong non-specific interactions with proteins (*13-18*).

We and others have recently developed an approach for integrating biological molecules with carbon nanotube devices that is based on coating the CNTs with lipid bilayers (*19, 20*). In these devices, the lipid bilayer performs two key roles: it serves as an impenetrable barrier between the CNT and the surrounding medium turning it from a "bare" wire into a "shielded" wire, and it also serves as a matrix for membrane proteins. In this work, we have exploited these two key advantages to demonstrate a bionanoelectronic device that uses a protein machine, Na^+/K^+-ATPase, powered by ATP hydrolysis, to control the output of a carbon nanotube transistor. The Na^+/K^+-ATPase is an ion transporter protein found in virtually all eukaryotic cells (*8, 21*); its function is to control and maintain sodium and potassium ion gradients and osmotic pressure across the plasma membrane (*6, 7*). This protein uses ATP hydrolysis energy to undergo a cycle of conformational changes (*6, 7, 22*) that translocates three Na^+ ions and two K^+ ions in opposite directions across the membrane, with the net result of accumulating an extra cation at the extracellular side of the membrane (the side opposite to the ATP hydrolysis site). Specificity in controlling ionic gradients (*6, 23, 24*), simple reconstitution (*25, 26*), and abundance in nature make Na^+/K^+-ATPase an attractive component for use in nanoelectronic devices. Several previous studies have integrated biological components with nanotube or nanowire electronic devices (*20, 27*). However, these devices incorporated passive biological components, which transmitted an environmental change to the nanowire using molecular recognition (*20*), or equilibrium ion transport (*27*). Our work demonstrates the possibility of integrating an actual powered biological machine, which could actively control the output of the electronic circuit. The ability to use powered biological components is significant, as they play a key role for most cellular processes; for example, recent modeling studies indicate that use of active ion pumps is necessary for biomimetic voltage generation (*28*).

Our experiments used a carbon nanotube transistor platform (Fig. 1a, also see *Supplementary Materials* for more details), in which a single semiconducting single-walled carbon nanotube bridged two metal electrodes that served as transistor's source and drain (Fig. 1a,b). The source and drain electrodes were insulated from the solution by an

additional coating with LOR3A photoresist that left only the middle section of the CNT exposed to the solution. This modification not only improved the signal to noise ratio, but also eliminated any contribution from the nanotube-electrode contacts (*15, 18, 29*). We used vesicle fusion to coat the device surface with a lipid bilayer that incorporated reconstituted Na^+/K^+-ATPase molecules. Finally, we covered the device with a PDMS microchannel that delivered ATP solution to power the ion pump. The gate voltage was applied by a reference Ag/AgCl microelectrode inserted in the PDMS fluid cell.

When we coated the CNT devices with the lipid bilayer that did not incorporate any membrane protein molecules, the device threshold voltage shifted by 250mV to more negative values (Fig. 1c), consistent with the distribution of changes in lipid headgroups (*20*). The shape of the IV curve remained unchanged, indicating that lipid coating did not decrease the performance of the carbon nanotube transistor. Surface Plasmon Resonance experiments indicated that the lipid membrane consisted of a single bilayer (thickness 6.3 nm). Further characterization with fluorescence recovery after photobleaching (FRAP) showed that the lipid bilayer fused on the device surface was mobile, similar to the results obtained previously (*20*). Critically, the cyclic voltammetry measurements using individual metallic carbon nanotubes as working electrodes (Fig. 1d) showed that lipid bilayer created an insulating barrier that caused the redox current observed in these experiments to drop by more than 84%. This value compares well with the 95%~97% drop recorded for lipid bilayers supported on metal electrodes (*30-34*) as well as 85%~95% drop reported for lipid bilayers on nanowire electrodes (*35*). This observation confirms that lipid bilayer forms an effective transport barrier between the nanotube surface and solution species.

When the lipid bilayer covering the CNT incorporates functional Na^+/K^+-ATPase molecules (Fig. 1a) we expect that the ion pump activity would induce ion transport across the membrane and alter the electric field around the carbon nanotube. This field would then modulate the transistor's source-drain current. Indeed, when we flowed 10mM ATP solution through the device that contained Na^+/K^+-ATPase molecules in the lipid bilayer (we confirmed that the pump was hydrolyzing ATP with a colorimetric assay, see *Supplementary Materials* for details), we observed that the CNT transistor conductance showed a sharp increase of about 35% (Fig. 2a). The IV_g curve measured in presence of ATP also shifted relative to the IV_g curve measured in pure buffer solution, yet the overall shape of the curve remained unchanged, indicating that the cause of the observed effect was gating of the CNT (*29*). The conductance change triggered by addition of ATP was

reversible: the device conductance returned to the original level when we replaced ATP solution with the buffer solution (Fig. 2a). A control experiment using the same device setup without the Na^+/K^+-ATPase protein did not yield any significant changes in the IV_g curve (Fig. 2a). Device conductance was also unaffected by an increase in the concentration of the ATP hydrolysis products, ADP and phosphate ion. Exposure to the solutions of non-hydrolyzable ATP analogs β,γ-methyleneadenosine 5′-triphosphate and adenosine 5′-[γ-thio]triphosphate also did not produce an increase in conductance (see *Supplementary Materials*) excluding the possibility that simple binding of ATP to the protein caused the conductance change. These control experiments confirm that the observed rise in device current in presence of ATP is likely a direct result of the ion pump transporting the ions across the lipid membrane.

The preparation method that we used to generate the lipid bilayers does not control the orientation of the protein in the membrane; therefore we expected that both possible orientations of the protein— ATP-site-up and ATP-site-down— will be present in the bilayer covering the devices (*25*). However, the barrier properties of the lipid bilayer should ensure that only the protein in the ATP-site-up configuration (i.e. the ATP hydrolysis site facing the outer side of the membrane) would produce measurable device activity. We verified this conclusion using two Na^+/K^+-ATPase inhibitors— ouabain, which inhibits its activity by binding to the protein on its extracellular side (the membrane side opposite the ATP hydrolysis side) (*36, 37*), and vanadate ion that competitively inhibits ATP hydrolysis by binding to the cytosolic side of the ATPase (*38*). Indeed, addition of 10 mM ouabain to the ATP solution had negligible effect on the device response; in contrast, addition of the 10 mM vanadate ion inhibited the protein activity almost completely (Fig. 2b). These results confirm that the ATP-dependent nanotube conductance increase is caused by specific activity of the Na^+/K^+-ATPase, and that only the proteins whose ATP-binding site is facing outside the device contribute to the measured signal.

To study the effect of the specific activity of the protein further we measured the device response at different ATP concentrations. Carbon nanotube transistors responded to the ATP concentrations of 1mM and above with the magnitude of conductance jump increasing and reaching saturation at ATP concentrations above 10mM (Fig. 3a). The observed relationship between the pump activity and ATP concentration follows the classic Michaelis-Menten enzyme kinetics (Fig. 3b) with the Michaelis-Menten constant, K_m, of 2.8 mM. This value is larger than the K_m values obtained for Na^+/K^+-ATPase activity in

microsomes (0.1∼0.5 mM) (*37, 39*) and in vesicles (13 μM) (*40*). We believe that the reduced activity observed in our experiments could be due to the extreme proximity of the protein tail to the device surface. γ-subunit of Na^+/K^+-ATPase extends at least 1-2 nm into extracellular space (*41*) while the thickness of the water cleft between supported lipid bilayer and the substrate was measured as 1.7 nm (*42*).

It is tempting to assign the observed nanotube conductance changes to the direct gating of the CNT transistor by the transmembrane potential developed by the electrogenic operation of the Na^+/K^+-ATPase. However, a closer look suggests a more complicated mechanism. The buildup of positive ions (Fig. 1a) should shift the effective gate voltage to more positive values and produce a *reduction* in the device current instead of the current *increase* observed in our experiments. To explain the device response we need to consider the possibility that pumping of excess cations to the bilayer inner surface could change the ion equilibrium and increase pH in an aqueous layer between the lipid bilayer and the device surface; indeed alkalinization of the vesicles containing working Na^+/K^+-ATPase has been reported (*43, 44*). To provide direct evidence for this hypothesis, we have tested whether Na^+/K^+-ATPase action causes alkalinization of the space between lipid bilayer and the substrate in our experiments. For these measurements we used lipid bilayers doped with a small amount of lipid conjugated at the headgroup with a fluorescein derivative dye (FITC) that acted as a pH reporter. When this dye-doped bilayer containing the Na^+/K^+-ATPase was exposed to the ATP solution, the dye fluorescence increased (Fig. 3c) indicating that the protein activity does raise the pH on the opposite side of the lipid bilayer. A comparison of these data with a calibration curve (see *Supplementary Materials*) estimates this pH increase to be about 1.3 units.

Uncoated CNT transistors also displayed a significant sensitivity to solution pH, with the nanotube conductance increasing steadily with pH≥7 (Fig. 3d). A recent study reported that graphene transistor conductance increased with the increase in pH, possibly due to the adsorption of hydroxyl ions (*45*); a similar mechanism could also work for carbon nanotubes (*46*). Another possibility is that a pH change ionizes silanol groups and creates negative charges close to the CNT surface that shift device conductance (*47*). The data on Fig. 3d indicate that ∼1.37x conductance increase observed when we exposed the devices to 10mM ATP solution corresponds to the pH change of about 1.6 units. This estimate agrees well with the estimate of a pH shift of 1.3 obtained from the fluorescence measurements. These results provide a strong indication that Na^+/K^+-ATPase-induced alkalinization of the

thin cleft between the bilayer and nanotube surface could indeed be the main process that causes the nanotube conductance increase. We note that the actual device response could also reflect a contribution from the membrane potential developed by the pump.

Finally, we want to discuss the kinetics of the device operation. After the pump becomes active, the transistor current increases and then reaches a steady-state plateau (Fig. 2a, 3a). This saturation could be caused either by a presence of a small leak through the pump or the lipid bilayer, or by a decrease in the pumping rate of the protein associated with the buildup of the membrane potential (*48*). If the last suggestion were true, then all time traces would have saturated at a similar level, independent of the ATP concentration; data on the Fig. 3a clearly contradict this suggestion, leading us to conclude that the saturation is likely caused by a leak through the device membrane. Indeed, further analysis (see *Supplementary Materials*) shows that observed kinetics is consistent with a simple kinetic model that incorporates a single leakage pathway. This model also explains why the ATPase-driven devices could function reliably in such seemingly imperfect configuration: as long as the pump activity was high enough to overcome the leakage rate, the devices produced a measurable response. This built-in robustness coupled with the ability for these devices to function in most biological environments, and the adaptability of lipid membranes as a scaffold for other biological systems provides a virtually unlimited opportunity for building more complex and sophisticated hybrid bionanoelectronic devices and circuits utilizing this platform.

Acknowledgements. A.N. acknowledges support from BES Biomolecular Materials Program and from UC-LLNL Research Program. A.A. , S-C.H. and J.M. acknowledge support from the LLNL LSP program. Parts of this work were performed under the auspices of the U.S. Department of Energy by Lawrence Livermore National Laboratory under Contract DE-AC52-07NA27344.

References

1. A. Goel, R. D. Astumian, D. Herschbach, *Proceedings Of The National Academy Of Sciences Of The United States Of America* **100**, 9699, (2003).
2. C. Bustamante, Z. Bryant, S. B. Smith, *Nature* **421**, 423, (2003).
3. M. V. Rodnina, W. Wintermeyer, *Annual Review Of Biochemistry* **70**, 415, (2001).
4. J. P. Caviston, E. L. F. Holzbaur, *Trends In Cell Biology* **16**, 530, (2006).
5. H. Hess, J. Clemmens, D. Qin, J. Howard, V. Vogel, *Nano Letters* **1**, 235, (2001).
6. H. J. Apell, *Bioelectrochemistry* **63**, 149, (2004).
7. P. L. Jorgensen, P. A. Pedersen, *Biochimica Et Biophysica Acta-Bioenergetics* **1505**, 57, (2001).
8. J. C. Skou, M. Esmann, *Journal of Bioenergetics and Biomembranes* **24**, 249, (1992).
9. A. Goel, V. Vogel, *Nature Nanotechnology* **3**, 465, (2008).
10. C. D. Mao, W. Q. Sun, Z. Y. Shen, N. C. Seeman, *Nature* **397**, 144, (1999).

11. I. Willner, E. Katz, *Bioelectronics: from theory to applications*. (Wiley-VCH, Weinheim, ed. 1st, 2005).
12. E. D. Minot *et al.*, *Applied Physics Letters* **91**, (2007).
13. S. S. Karajanagi, A. A. Vertegel, R. S. Kane, J. S. Dordick, *Langmuir* **20**, 11594, (2004).
14. M. Zheng *et al.*, *Science* **302**, 1545, (2003).
15. I. Heller, J. Mannik, S. G. Lemay, C. Dekker, *Nano Letters* **9**, 377, (2009).
16. K. Bradley, A. Davis, J. C. P. Gabriel, G. Gruner, *Nano Letters* **5**, 841, (2005).
17. H. Shimotani *et al.*, *Applied Physics Letters* **88**, (2006).
18. J. Mannik, I. Heller, A. M. Janssens, S. G. Lemay, C. Dekker, *Nano Letters* **8**, 685, (2008).
19. A. B. Artyukhin *et al.*, *Journal of the American Chemical Society* **127**, 7538, (2005).
20. X. Zhou, J. M. Moran-Mirabal, H. G. Craighead, P. L. McEuen, *Nature Nanotechnnology* **2**, 185, (2007).
21. J. C. Skou, *Biochimica Et Biophysica Acta* **23**, 394, (1957).
22. T. Shinoda, H. Ogawa, F. Cornelius, C. Toyoshima, *Nature* **459**, 446, (2009).
23. H. J. Apell, B. Bersch, *Biochimica Et Biophysica Acta* **903**, 480, (1987).
24. L. T. Buck, P. W. Hochachka, *American Journal Of Physiology* **265**, R1020, (1993).
25. F. Cornelius, J. C. Skou, *Biochimica Et Biophysica Acta* **772**, 357, (1984).
26. Jorgense.Pl, *Biochimica Et Biophysica Acta* **356**, 36, (1974).
27. N. Misra *et al.*, *Proc. Natl. Acad. Sci. USA* **106**, 13780, (2009).
28. J. Xu, D. Lavan, *Nature Nanotechnology* **3**, 666, (2008).
29. I. Heller *et al.*, *Nano Letters* **8**, 591, (2008).
30. A. Wardak, H. T. Tien, *Bioelectrochemistry And Bioenergetics* **24**, 1, (1990).
31. D. L. Jiang, P. Diao, R. T. Tong, D. P. Gu, B. Zhong, *Bioelectrochemistry And Bioenergetics* **44**, 285, (1998).
32. T. Martynski, H. T. Tien, *Bioelectrochemistry And Bioenergetics* **25**, 317, (1991).
33. H. T. Tien, S. H. Wurster, A. L. Ottova, *Bioelectrochemistry And Bioenergetics* **42**, 77, (1997).
34. H. T. Tien, A. L. Ottova, *Electrochimica Acta* **43**, 3587, (1998).
35. J. A. Martinez *et al.*, *Nano Letters* **9**, 1121, (2009).
36. D. Charlemagne, J. M. Maixent, M. Preteseille, L. G. Lelievre, *Journal Of Biological Chemistry* **261**, 185, (1986).
37. A. H. Neufeld, H. M. Levy, *Journal Of Biological Chemistry* **244**, 6493, (1969).
38. S. J. D. Karlish, L. A. Beauge, I. M. Glynn, *Nature* **282**, 333, (1979).
39. M. Yamaguchi, Y. Tonomura, *Journal Of Biochemistry* **88**, 1377, (1980).
40. H. J. Apell, V. Haring, M. Roudna, *Biochimica Et Biophysica Acta* **1023**, 81, (1990).
41. J. P. Morth *et al.*, *Nature* **450**, 1043, (2007).
42. V. Kiessling, L. K. Tamm, *Biophysical Journal* **84**, 408, (2003).
43. C. Polvani, R. Blostein, *Journal of Biological Chemistry* **263**, 16757, (1988).
44. S. Schlemmer, F. Sirotnak, *Journal of Biological Chemistry* **267**, 14746, (1992).
45. Y. Ohno, K. Maehashi, Y. Yamashiro, K. Matsumoto, *Nano Letters*, ASAP, (2009).
46. H. Pan, Y. Feng, J. Lin, *Physical Review B* **70**, 245425, (2004).
47. A. B. Artyukhin *et al.*, *Nano Lett.* **6**, 2080 (2006).
48. F. Cornelius, *Biochimica Et Biophysica Acta* **1071**, 19, (1991).

FIGURES

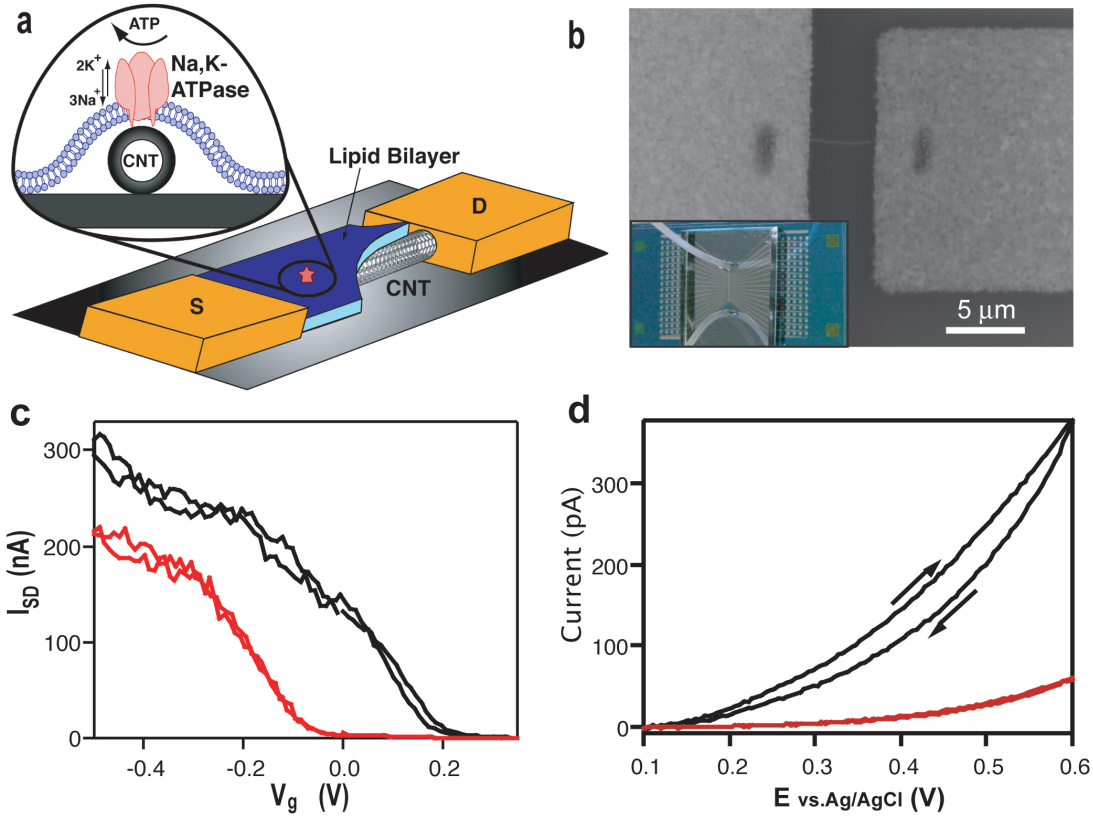

Figure 1. **(a)**. Schematics of the experimental setup. A single carbon nanotube bridges source (S) and drain (D) electrodes of a microfabricated transistor device. The nanotube is covered by a lipid bilayer that incorporates a Na^+/K^+-ATPase ion pump. **Inset**: A cross-section of the device showing the nanotube, lipid bilayer, the protein, and directions of the ion fluxes. **(b)**. An SEM image of the source-drain region of the CNT transistor showing a nanotube bridging two electrodes. The image was taken before the application of the protective LOR3A coating. **Inset**: A photograph of the 2cmx1cm device chip covered with a PDMS microfluidic channel. **(c)**. IV_g curve recorded for a bare CNT device (black trace) and a device covered with a lipid bilayer (red trace). **(d)**. Cyclic voltammetry curves recorded in 10mM $K_4Fe(CN)_6$ solution using a carbon nanotube as a working electrode for a bare CNT device (black trace) and a CNT device covered with a lipid bilayer (red trace).

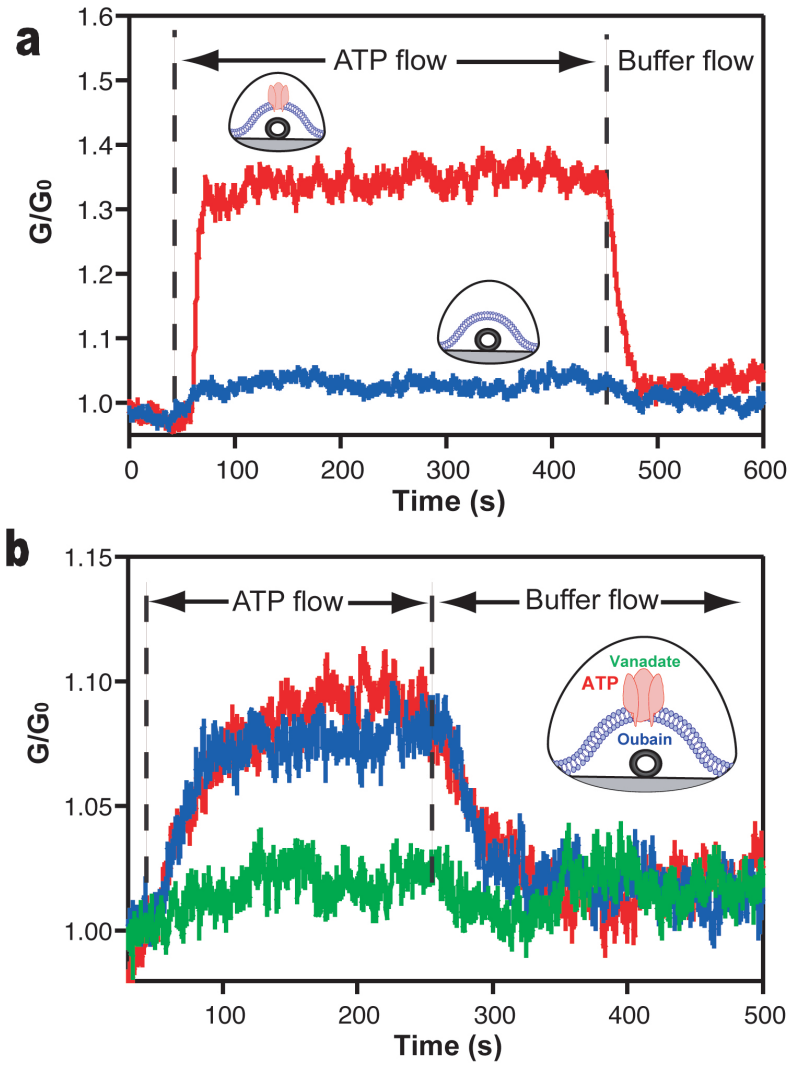

Figure 2. **(a)**. Time traces of normalized nanotube conductance recorded for the devices covered with a lipid bilayer incorporating Na^+/K^+-ATPase (red trace) before, during, and after injection of 10 mM ATP solution in the cell. Blue trace shows the response of a similar device that did not have protein in the lipid bilayer. The applied gate voltage V_g = -0.05V. **(b)**. Time traces of normalized conductance of the Na,K-ATPase containing device in response to introduction of a 10 mM ATP solution (red), and a mixture of 10 mM ATP and Na,K-ATPase inhibitors, 10 mM oubain (blue) and 10 mM sodium vanadate (green). The applied gate voltage was V_g =-0.4V.

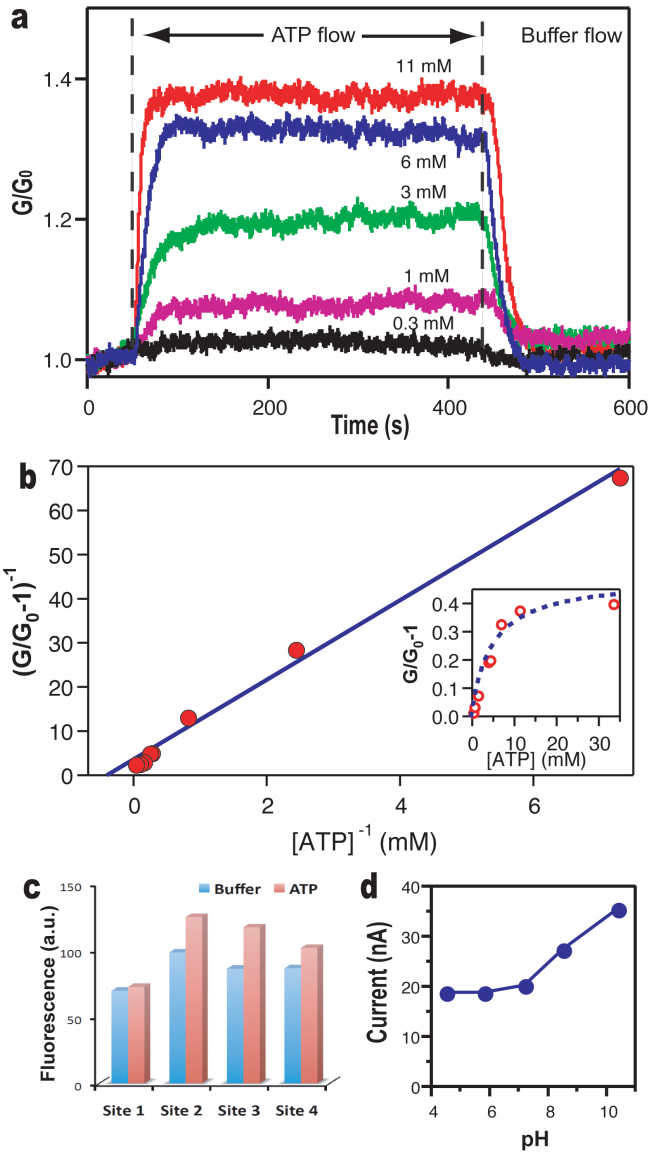

Figure 3. (a). Time traces of normalized conductance of the Na^+/K^+-ATPase containing CNT device recorded at different concentration of ATP as indicated on the plot. The applied gate voltage was V_g = -0.2V. **(b)**. Lineweaver–Burk (double reciprocal) plot of the reaction rate (expressed as relative conductance increase, G/G_0-1) as a function of the ATP concentration. The intercept estimates the value of the Michaelis constant as K_m=2.8mM. Inset shows the regular Michaelis-Menten plot of the same data. Blue lines on the main plot and on the inset represent the fit of the data to the Michaelis-Menten equation: $P = P_0 \frac{[ATP]}{[ATP] + K_m}$. **(c)**. Fluorescence intensity measured for a lipid bilayer doped with a pH-sensitive dye (FITC)

and incorporating Na^+/K^+-ATPase. Bar chart shows fluorescence intensity measured on four different sites on the surface first in pure buffer (blue bars) and then in buffer/ATP mixture (red bars). High fluorescence level corresponds to higher pH values. **(d)**. Source-drain current of the uncoated CNT transistor recorded at different pH values of the buffer solution. The applied gate voltage was V_g=-0.17 V.